

PRELIMINARY RESERVOIR AND SUBSIDENCE SIMULATIONS FOR THE AUSTIN BAYOU
GEOPRESSED GEOTHERMAL PROSPECT*

S. K. Garg, T. D. Riney and D. H. Brownell, Jr.
Systems, Science and Software, La Jolla, California

For the last several years, the University of Texas at Austin (UTA) has analyzed the geopressed tertiary sandstones along the Texas Gulf Coast with the objective of locating prospective reservoirs from which geothermal energy could be recovered. Of the "geothermal fairways" (areas with thick sandstone bodies and estimated temperatures in excess of 300°F), the Brazoria fairway appears **most** promising and the Austin Bayou Prospect has been developed within this **fairway**.¹ A test well (DOE 1 Martin Ranch) is currently being drilled in this area. Pending the availability of actual well test data, estimated reservoir properties have been employed in numerical simulations to study the effects of variations in reservoir properties on the projected long-term behavior of the Austin Bayou Prospect. The simulations assess the sensitivity of the reservoir behavior to variations in estimated sandstone/shale distribution, shale compressibility, and vertical shale permeability. Further, hypothetical properties for the stress-deformation behavior of the rock formations were employed in a very preliminary study of the potential ground surface displacements that might accompany fluid production.

AUSTIN BAYOU PROSPECT

It is estimated that the Austin Bayou Prospect has a total sandstone thickness of 800-900 ft, average permeability (from unconfined cores) of 40-60 md, fluid temperature in the range of 300°F (at 14,000 ft depth) to 350°F (at 16,500 ft), and salinities in the range of 40,000-100,000 ppm. It is estimated that the test well will drain several sandstone reservoirs (zones A, B, C, D, E and F in Figure 1) in an area of approximately 16 square miles.¹ The net sandstone thickness, inferred from an interpolated spontaneous potential log, is 840 ft. Average porosity of at least 0.20 is predicted for 250 ft of the sandstone; the remaining sandstone has a porosity of between 0.05-0.20 with an average value of 0.15. The total pore volume, water in pores, and gas in place are estimated to be 60 billion cubic ft, 10 billion bbl, and 426 billion cubic ft, respectively.

RESERVOIR RESPONSE CALCULATIONS

It is likely that the test well will first be used to produce from sand bodies located within a single zone; the simulations consider production to be entirely from Zone E which has the thickest sandstone bodies (50-100 ft). A series of four axisymmetric calculations was run

Work performed for UTA under DOE Contract EY-76-C-5040-1S.

with the ³ MUSHRM reservoir computer model to simulate the behavior of layered sandstone/shale sequences used to represent Zone E (Figure 1). MUSHRM includes treatment of all the important fluid/rock response mechanisms and their interactions, that are believed to be operative in Gulf Coast geopressured geothermal reservoirs.² The reservoir is assumed to be a cylindrical disc with radius $R = 3.63$ km (corresponding to a block area of 16 square miles) and height 152.4 m (500 ft, corresponding to the top and bottom of Zone E at depths of 15,300 and 15,800 ft, respectively). The net sand thickness (= net shale thickness) is 76.2 m (250 ft). The reservoir fluid is assumed to be liquid water saturated with methane. The initial pore pressure, temperature and methane mass fraction at a depth of 15,500 ft are 793 bars (11,500 psi), 162.7°C (325°F) and 0.007, respectively. The reservoir fluid is assumed to be initially in hydrostatic equilibrium so that the initial values of pore pressure and methane mass fraction vary slightly over the 500 ft reservoir thickness. The reservoir is produced at a constant mass rate of 36.8 kg/sec (20,000 STB/day); all of the production is from the sandstone layers.

For the sandstone layers we assume horizontal permeability = 20 md; vertical permeability = 2 md; grain density of rock = 2.63 g/cm³; initial porosity of rock = 0.20; rock thermal conductivity = 5.25 ergs/sec-cm-°C; rock specific heat = 0.963×10^7 ergs/g-°C; rock bulk compressibility = 7.25×10^{-9} cm²/dynes; irreducible liquid saturation = C.3 and irreducible gas saturation = 0.0. The latter two parameters define the relative permeabilities, in the case of two-phase flow, using the Corey formulation. For the shale layers we assume identical properties as for the sand layers except for horizontal permeability, vertical permeability and rock bulk compressibility. These properties, as well as the sequencing of the sandstone/shale layers, are varied in the four MUSHRM calculations.

Figure 2 shows the numerical grid, along with the sandstone/shale arrangement, used in simulation #1 (base case). In simulation #2 (thick sands), the arrangement shown in Figure 3 was used. For these two cases the shale layers are assumed to have horizontal permeability = 10^{-4} md; vertical permeability = 10^{-5} md; rock bulk compressibility = 14.5×10^{-10} cm²/dynes. Simulation #3 (high shale k_v) is the same as #1 except the vertical permeability of the shale layer is increased ten-fold to 10^{-4} md. Simulation #4 (small shale C) is the same as #1 except the bulk rock compressibility of the shale layers is decreased ten-fold to 14.5×10^{-11} cm²/dynes.

Figure 4 shows the time-dependent pressure decline in the various sandstone well-blocks for all four MUSHRM simulations. For simulation #1 (base case) the pressure drops in well-blocks ($i = 1, j = 2, 4, 9$) are essentially the same but differ substantially from those in well-blocks ($i = 1, j = 6, 7$). This clearly illustrates the influence of fluid influx from the adjoining shales. Layers $j = 2, 4, 9$ are each a 50 ft thick sandstone body sandwiched between shale layers, whereas layers $j = 6, 7$ are contiguous sandstone bodies with a total thickness of 100 ft. We further note, however, that the pressure drop for all of the sandstone layers is very nearly identical for the first year or two; influx from

adjoining shales should have little or no effect for practical drawdown/buildup times employed in well testing.

Simulation #2 (thick sands) uses the same estimated properties for the sandstone and shale layers as for the base case, but the net sandstone of 250 ft is a single thick body sandwiched between 125 ft thick shale bodies. As shown in Figure 4, the pressure drops in the sandstone layers comprising the 250 ft thick body are essentially identical. The drop is nearly the same as for simulation #1 (base case) for $t < \sim 2$ years; this again indicates that the fluid influx from shale layers will be important only for long production times. For $t > \sim 3$ years, higher pressure drops are obtained for simulation #2 (thick sands); the importance of fluid influx from the shales decreases with increasing sandstone thickness. Comparison of simulation #3 (high shale k_v) with the base case shows that the ten-fold increase in the vertical permeability of the shale layers enhances the fluid influx and thus greatly reduces the long-term pressure drop in the sandstone well-blocks (Figure 4). Nevertheless, the influence of the influx is minimal for $t < \sim 1$ year. Finally, comparison of the results for simulation #4 (small shale C) with the base case shows that a ten-fold decrease in the bulk rock compressibility of the shale layers causes a larger pressure drop in the sandstone well-blocks; this effect, however, becomes evident only for $t > \sim 10$ years.

The **MUSHRM** simulator computes porosity along with the fluid state in each computational cell at each stage of a calculation. Given current and initial porosities, the radial variation of the vertical compaction of the reservoir may be computed; the compaction at $t = 30.3$ years is depicted in Figure 5 for each of the four reservoir simulations.

PRELIMINARY SUBSIDENCE STUDIES

Estimation of the vertical (subsidence) and horizontal movements of the ground surface that might accompany reservoir compaction requires knowledge of the stress-deformation behavior of the rock units constituting the reservoir (Zone E) and the overlying and underlying strata. Since such data were not available, hypothetical properties were used in the ³AGRESS simulator which couples the reservoir response model (**MUSHRM**) with a rock stress-deformation response model.² Figure 6 shows an axial section of the configuration treated. The test well is expected to enter the geopressured zone at a depth of approximately 10,000 ft. Rocks are likely to be competent in the geopressured zone; above that depth the rocks may be unconsolidated. Accordingly, the formation properties of the rocks surrounding the reservoir are permitted to be different in Region I (depth $< 10,000$ ft) and Region II (depth $> 10,000$ ft) for the ground movement studies.

We assume that the Zone E sandstone/shale layer arrangement, formation properties, initial fluid state, and the imposed fluid production are identical to those used for reservoir simulation #1 (base case). In addition to the reservoir formation properties given earlier, we assume

the following stress-deformation properties for the reservoir sandstone (shale) layers: bulk modulus of porous rock = 9.20 kb (0.46 kb); shear modulus of porous rock = 3.45 kb (0.17 kb); bulk modulus of rock grain = 300 kb (100 kb). Since the reservoir pore pressure declines monotonically during fluid production, the values selected are for loading conditions. The overburden/underburden rocks are assumed to be linearly elastic; three parametric AGRESS simulations were made to assess the effects of variations in rock properties. Case A (soft) treats both Region I and Region II as unconsolidated rock with bulk modulus = 25 kb and shear modulus = 9.375 kb. Case B (mixed) treats Region I the same as Case A, but assumes the geopressured zone is four times as stiff (Region II bulk modulus = 100 kb and shear modulus = 37.5 kb). In Case C (stiff), both Region I and Region II are treated as competent rock (i.e., bulk modulus 100 kb and shear modulus = 37.5 kb).

The surface vertical and horizontal movements calculated by the three AGRESS simulations at $t = 30.3$ years are shown in Figure 7. The horizontal movement is directed toward the test well ($r = 0$). The combined effect of the movements is to form a subsidence bowl. The main effect of an increase in rock stiffness is to reduce the surface displacements. Comparison of Figures 5 and 7 shows that only a small fraction of the reservoir compaction is calculated to appear as surface subsidence.

CONCLUDING REMARKS

The parametric geopressured reservoir simulations strongly suggest that for sandstone thicknesses greater than 50 ft, the effect of shale fluid influx will not be felt for production times less than one to two years. This implies that the effect can be ignored for drawdown/buildup times practical in well testing, but the influx from shales will likely play an important role in determining long-term pressure drop in the sandstones, and also in the associated reservoir compaction. The parametric ground surface displacement simulations suggest that only a fraction of the reservoir compaction will appear as surface subsidence. It should be emphasized that the estimated values for reservoir properties used in the reservoir response calculations must be confirmed by data from the DOE 1 Martin Ranch test well. The preliminary calculations for the ground surface movements are even more tenuous since they are based upon hypothetical overburden/underburden rock properties.

REFERENCES

1. Bebout, D. G., R. G. Loucks and A. R. Gregory, "Study Looks at Gulf Coast Geothermal Potential," Oil and Gas Journal, September 26, 1977. "Texas Geothermal Prospect Slated to Begin Operations at Martin Ranch," Oil and Gas Journal, October 3, 1977.
2. Garg, S. K., J. W. Pritchett, D. H. Brownell, Jr., and T. D. Riney, "Geopressured Geothermal Reservoir and Wellbore Simulations," Systems, Science and Software, La Jolla, California, Report SSS-R-78-3639, 1978.

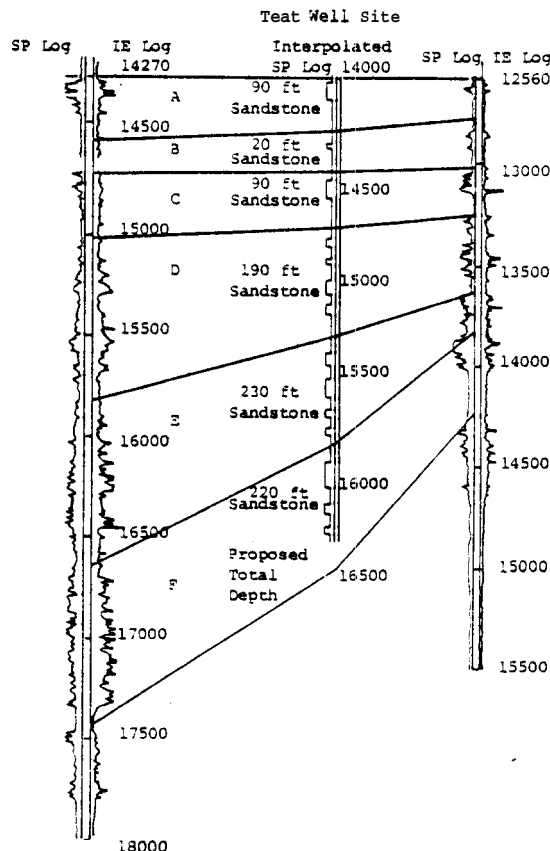


Figure 1. Expected sandstone distribution for the test well site from a synthetic SP log created by interpolation from existing control wells (from Bebout, et al.).

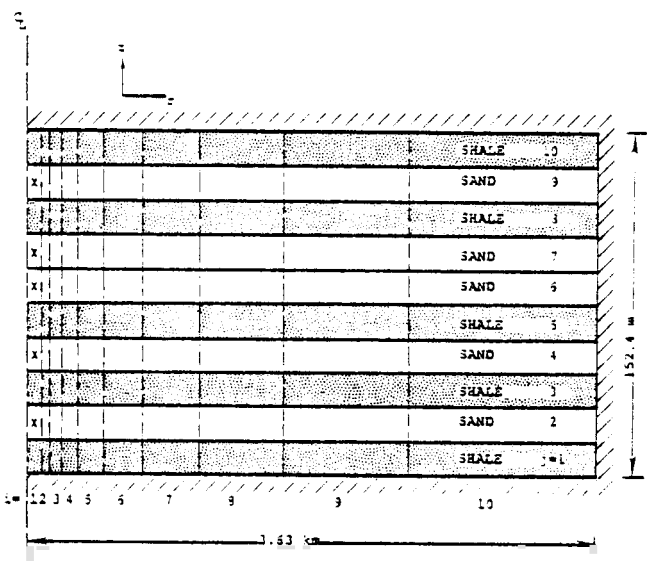


Figure 2. Axial section of the numerical grid and the shale/sandstone arrangement utilized in Cases 1, 3 and 4. The well-blocks from which fluid is produced are indicated by X.

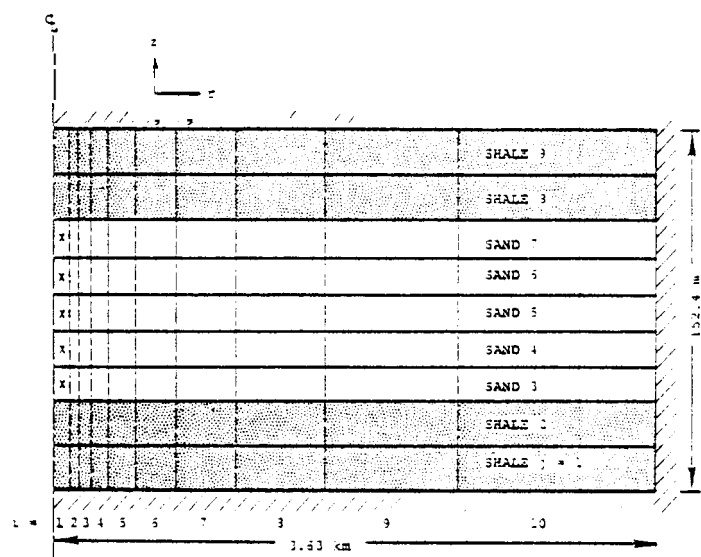


Figure 3. Axial section of the numerical grid and the shale/sandstone arrangement utilized in Case 2. The well-blocks are indicated by X.

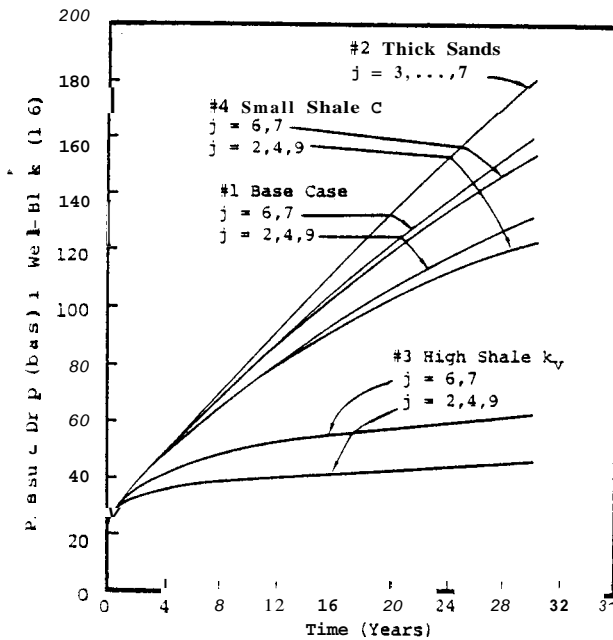


Figure 4. Pressure drop in sandstone well-blocks ($i = 1$).

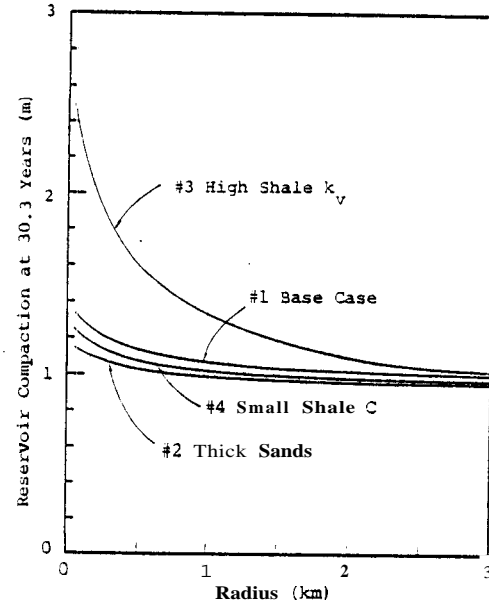


Figure 5. Radial distribution of the vertical compaction of the reservoir.

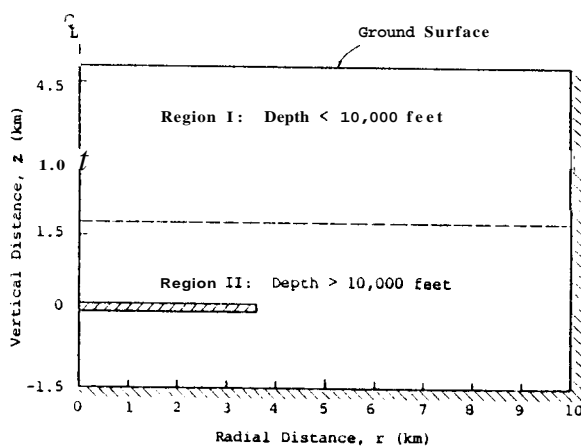


Figure 6. Axial section showing the reservoir (hatched) and the surrounding rocks. Both the bottom and the right vertical (i.e., $r=10$ km) boundaries are assumed to be fixed.

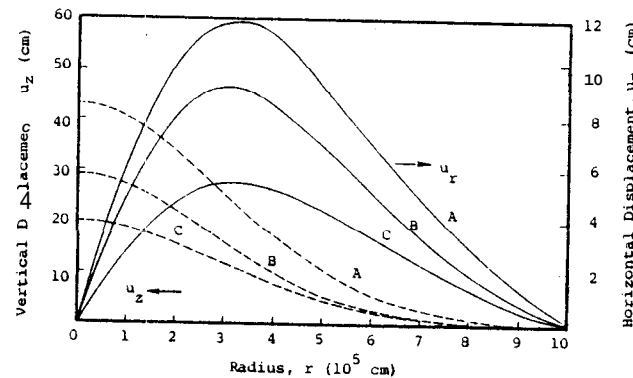


Figure 7. Surface vertical displacement (left) and horizontal displacement (right) at $t = 30.3$ years for three choices of rock elastic properties.